

## BASALT FIBER AS A REINFORCEMENT OF POLYMER COMPOSITES

Tibor CZIGÁNY\*, János VAD\*\* and Kornél PÖLÖSKEI\*

\*Department of Polymer Engineering  
Faculty of Mechanical Engineering  
Budapest University of Technology and Economics  
H-1111 Budapest, Műegyetem rkp. 3., Hungary  
e-mail: czigany@eik.bme.hu

\*\*Department of Fluid Mechanics  
Faculty of Mechanical Engineering  
Budapest University of Technology and Economics  
H-1111 Budapest, Bertalan L. u. 4-6., Hungary

Received: July 13, 2004

### Abstract

The applicability of basalt fibers as reinforcing materials has been examined in a polypropylene (PP) matrix. The brittle basalt fibers have been mixed with the PP fibers by carding combined with needle punching and the composite sheets have been produced by pressing. SEN-T fracture mechanical specimens have been cut out of the sheets and the sensitivity to crack propagation has been examined in the composites. It has been proven that fracture toughness increases as a result of reinforcing. The toughness of the composite increased compared to the matrix due to the gravels appeared at the end of basalt fibers. It has been pointed out that the gravels are results of the Junkers production technology. The observations have also been proven by electron microscopic images. A model has been outlined for investigation of influence of change of technological parameters on basalt fiber production.

*Keywords:* basalt fiber, fiber head, polypropylene composites, fracture toughness, model of basalt fiber production.

### 1. Introduction

The spread of polymer composite structural materials allows the development of products in all application fields that fulfil the technical requirements in the most effective way. The increasing economical and environmental demands on the reinforcements of load-bearing polymer structural materials encourage researchers to develop new, high-strength reinforcing materials and structures. As a consequence, in the last years intensive research has begun all over the world with regard to the applicability of different organic and inorganic reinforcing fibers in polymer matrices. Hence, basalt fiber of mineral origin has gained increasing attention as a reinforcing material compared to traditional glass and carbon fibers [1].

The basis of basalt fibers is basalt rock which is a volcanic, over-ground, effusive rock saturated with 45–52% SiO<sub>2</sub>. As a result of this formation, basalt has several advantageous properties. Besides its high modulus of elasticity and

excellent heat resistance, the fibers made of basalt have significant capability of heat and acoustic resistance and are outstanding vibration isolators. The good insulation property of basalt was recognized earlier, that is why it is a widespread insulation material in the construction industry, processed in the form of rockwool. The basis of rockwool is basalt fiber, the production of which is the following: basalt rock is melted and beaten into fibers in a way that fibers with the diameter of 7–13  $\mu\text{m}$  and a length of 60–100 mm are formed from the melt at a temperature above 1500°C by the means of a centrifugal blowing process. This material is used as insulator at constructions due to the fact that it is an excellent acoustic and thermal insulator and vibration damper, as well as non-flammable, chemically indifferent, resistant to corrosion and biologically stable.

Several articles dealing with glass and carbon fiber reinforced polymer composites mention the significance of basalt fiber as a possible new reinforcing material [2, 3]. With use of such low density and tough composites instead of metal raw materials e.g. in manufacturing of rotating fluid machinery mechanical problems e.g. related to swept rotor blades [4, 5] can be surmounted [6]. There are only a few researchers who managed to create a composite to embed basalt fibers in a polymer matrix [7, 8]. The main reason is the problem of fiber-matrix interfacial interaction and the high sensitivity to fracture in basalt fibers.

The aim of this paper is to study the applicability of basalt fibers as reinforcing materials in polymers, to determine the fiber properties and to outline a model for fiber production.

## 2. Experiments

### 2.1. Materials

The basalt fibers (TOPLAN, Hungary) used in the experiments were produced with the so-called Junkers technology. The principle of the Junkers technology is the following: the melted mineral mixture is run radially on high speed fiberization disks and the developing fibers are blown off by high velocity axial air jets acting near the circumference of the disks. This way of fiber spinning is especially productive, inexpensive, and provides a relatively even fiber quality. The disadvantage is that it provides a fiber assembly similar to cotton-wool that is difficult to be separated into fibers without major damage (fracture) in the fibers and that cannot be absorbed appropriately by a melted polymer matrix because of its compactness. Hence, the material of the matrix, polypropylene type PP100 TIPFIL (TVK, Hungary), has also been used in the form of fibers. In order to produce and examine a composite, sheets with 30 weight percent basalt fiber were pressed in a laboratory press type COLLIN P 200 T. The homogeneous mat that served as a basis for pressing was produced by a combined process of needle punching and carding. Since mineral fibers do not possess the characteristics of textiles, carrier PP fibers were used in the process. Carding was carried out on a multicylinder carding machine type

BEFAMA 3K, and the carded mat was needle-punched and packed afterwards. The advantage of the process is that it is productive and provides an even end-product. The disadvantage is that the brittle mineral fibers crack to small extent but this problem can be minimized by cylinder settings, when the too short fibers fall out at the overlaps between the cylinders. This latter fact must be taken into consideration when the adequate matrix-reinforcing fiber weight proportion is to be set.

## 2.2. Specimens and their Characterization

The material properties of the applied mineral and matrix fibers were measured with the help of a Projectina projection microscope, type 4014/BK-2, and a tensile testing machine type Zwick 1464 equipped with a fine extensometer according to the standard JIS R 7601.

In order to determine the critical stress intensity factor, SEN-T (Single Edge Notched Tensile) specimens notched on one side were used (for the dimensions see *Fig. 1*).

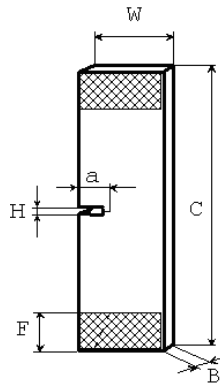


*Fig. 1.* SEN-T specimen, ( $W = 30$  mm,  $a = 10 + 1$  mm,  $B = 2$  mm,  $C = 110$  mm,  $F = 15$  mm,  $H = 1$  mm)

## 2.3. Fracture and Failure Behavior

The SEN-T specimens were tested on a ZWICK Z020 type universal tensile testing machine at a crosshead speed of 1 mm/min at ambient temperature (RT). The fracture toughness was determined on the basis of the load-elongation ( $F - \Delta l$ )

response of the SEN-T specimens:

$$K_c = \frac{F_{\max}}{B \cdot W} \cdot a^{1/2} \cdot f(a/W), \quad (1)$$

where:  $F_{\max}$  – maximum force in the  $F - \Delta l$  trace  
 $B$  – thickness of the specimen  
 $W$  – width of the specimen  
 $a$  – total notch length (produced by saw and razor blade)  
 $f(a/W)$  – geometrical correction factor

$$f(a/W) = 29.6 - 185.5(a/W) + 655.7(a/W)^2 - 1017(a/W)^3 + 638.9(a/W)^4. \quad (2)$$

Five specimens were tested in order to calculate the  $K_{IC}$  value and the specimen size parameters (i.e.  $a$ ,  $W$  and  $B$ ) were measured on each specimen.

### 3. Results and Discussions

#### 3.1. Fiber-Properties

*Table 1* contains the geometrical and mechanical properties of PP and basalt fibers. The table reveals the small strain of basalt fibers and the significant deviation of the dimensions. The latter fact is also confirmed by the distribution of the diameter of the basalt fibers (*Fig. 2*). The reason of the bimodal distribution is traceable to the manufacturing technology of the basalt fiber. The different revolution of the fiberization disks and the different viscosity of the melted layer formed in the disks cause the two peaks of the diagram (the detailed description can be found in chapter 3.3.).

*Table 1.* Characteristics of Polypropylene (PP) and Basalt Fibers

Fiber	Density [g/cm <sup>3</sup> ]	Length [mm]	Diameter [ $\mu$ m]	E modulus [GPa]	Elongation [%]	$\sigma$ tensile [MPa]
PP	0.91	100 $\pm$ 6	34.3 $\pm$ 4.2	4.2 $\pm$ 0.9	44.1 $\pm$ 16.2	331 $\pm$ 56
Basalt	2.70	80 $\pm$ 20	9.9 $\pm$ 2.6	63 $\pm$ 18	0.9 $\pm$ 0.3	571 $\pm$ 219

#### 3.2. Fracture Toughness

Five SEN-T specimens were cut out from each pressed sheet in the direction of the fibers and the sensitivity to crack propagation according to the *Eq. (1)* was examined.

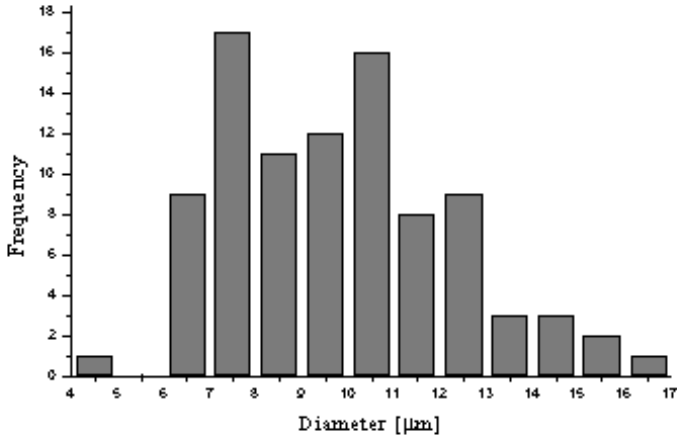
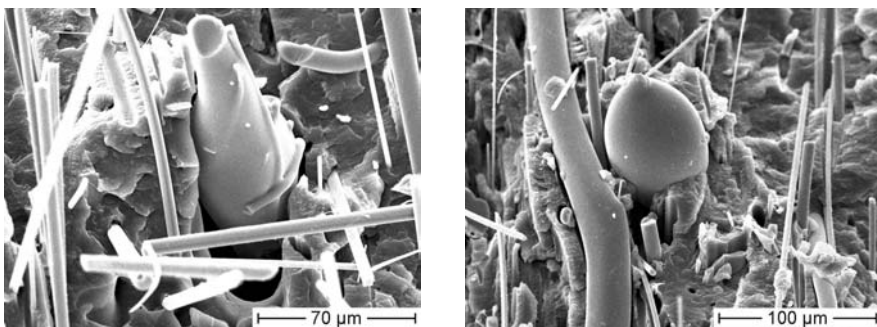


Fig. 2. Frequency of the diameter of basalt fibers

The  $K_{IC}$  values calculated from the measurement can be found in *Table 2*. The results show that the fracture toughness of the matrix can be increased by 20% with the help of the new reinforcing material. In order to obtain a more effective fiber-matrix adhesion the reinforcing and the PP fibers were treated separately. A peroxid solution (Luperox 101) was used in case of the matrix and glycerin monooleate (Priolube 1047) in case of basalt fibers [9]. It can be observed that the value of  $K_{IC}$  increased further as a result of the treatment. This is also proven by the acoustic activity during the tensile tests. The maximum value of the acoustic events that arose during loading of the untreated specimens was 50 dB. This value refers to fiber-matrix debonding and fiber pullout [10]. Besides the 50 dB signs 80-90 dB signs were also detected during the tensile tests of treated specimens. This means that fiber breakage occurred in the latter case and hence the increased fiber-matrix interfacial adhesion is proven. As a consequence of the embedment of the basalt fibers in the matrix, a non-expected, very high increase in plastic deformation has been experienced in the composite compared to the matrix. A possible explanation of this phenomenon is that the ends of the basalt fibers serve as stress concentration points and cause micro cavity formations in PP. The distribution of cavities is so even that they cause further matrix deformation that is revealed macroscopically by the observed toughness. As a proof, scanning electron microscopic (SEM) images were taken from the composite fracture surfaces (*Fig. 3*). The pictures reveal the spheres, which were supposed to be air bubbles, but turned out to be ‘fiber heads’ (gravels) remained from the fiber production. These gravels may be torn off or may stay on the end of the fiber because of the production technology. The fibers being formed cool down gradually and smaller or larger gravels remain on their ends depending on the length of the fibers. Most of the gravels break down during

deposition but the smaller ones remain on the fibers. During composite production further gravels heads break down and fall out of the mat as an effect of carding and needle punching but a small amount stays in the composite. In case of traditional reinforcing fibers fiber pullout is a frequent phenomenon [11] (*Fig. 4a*), but in case of basalt fibers produced by the Junkers technology gravels remaining on the fibers cause an increase in toughness because the gravels with larger diameter do not allow fiber pullout and the matrix deforms plastically (*Fig. 4b*). The broken-down gravels serve as initiation points for cracks as filling material (weak point).



*Fig. 3.* SEM picture of the presence of fiber heads (gravels) in the composite

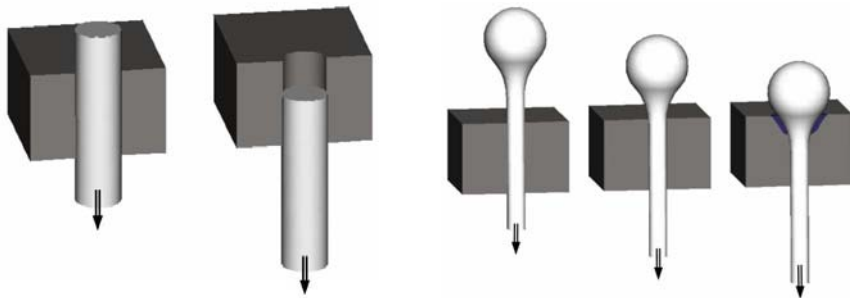


*Fig. 4.* a) fiber pullout from the matrix without fiber head, b) model of the toughness increase caused by fiber head during fiber pullout

The production of basalt fibers with more or less gravels is attempted by the further examination of gravels and the optimization of the technology (further modification of the e.g. temperature of the melt, disk speed, air flow rate etc.). The reason is that basalt fibers having gravels of nearly uniform size embedded in composites improve the mechanical properties of the latter and the increased toughness means improved impact resistance, in other words higher energy absorption capacity that is essential in case of products for instance in the automotive industry (e.g. bumpers). The reinforced concrete serves as an analogy because the ends of

Table 2. Fracture toughness in case of the matrix, 30 weight percent reinforcement content and with added treating agents

	PP	PP/Basalt	Treated PP/Basalt
$K_{IC}$ [MPa · m <sup>1/2</sup> ]	4.99±0.20	5.97±1.21	6.49±0.86

the steel wires are bent back before embedding them in concrete and this way they increase the strength of the reinforced concrete and decrease the risk of steel wire pull-out.

### 3.3. Modelling of Basalt Fiber Production

In this section, a combined fluid mechanical – thermodynamic model is outlined for the basalt fiber production. The model aims at providing guidelines how the parameters of the Junkers technology (i.e. basalt melt temperature, r.p.m. of fiberization disks, velocity of air jets etc.) influence the geometry of basalt fibers produced.

The formation of basalt fibers is a very complex process. The basalt melt originated from the gas-heated furnace operating at melting temperature of approx. 1580 °C is lead to a fiberization equipment comprising three rotating disks of horizontal axis (Fig. 5a). First the melt is run to an accelerating disk of smaller diameter and higher speed. The accelerating disk forwards the melt to two consecutive fiberization disks (Fig. 5b). A melt layer develops on the surface of the fiberization disks. The fiber formation process shows certain analogy with the operation of rotary disk atomizers. Due to the centrifugal forces, droplets protrude from the melt layer. When reaching a critical size, the droplets are detached from the disks, hauling fibers along.

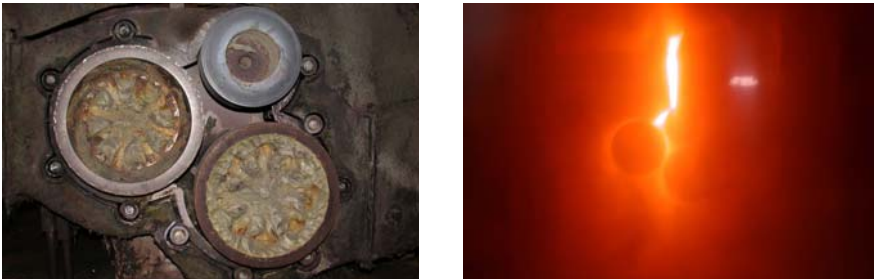


Fig. 5. a) the process of fiber spinning, the accelerating disk is above, the centrifugal disks are below, b) formation of a melt film

When discussing this process, the following components of the droplet/fiber ensemble are defined:

- Initial droplet: the droplet of critical size at the time instance of detachment from the fiberization disk,
- Gravel: the remainder of the initial droplet being diminished during the fiber formation process,
- Fiber: the component connecting the gravel to the location of its origin (location of the initial droplet).

The fiber formation can be modelled using basic fluid mechanical [12] and thermodynamic [13] laws. The modelling steps are outlined as follows:

- The initial droplet size is determined using the law of hydrostatics.
- Law for conservation of mass applies. With assumption of constant melt density, it is assumed that the volume of initial droplet is equal to the sum of volumes of gravel and fiber (no melt is supplied to the fiber from the melt layer on the disk after detachment of the initial droplet).
- The instantaneous position of the gravel (modelled as a lumped parameter element) is determined from its equation of motion, including centrifugal and Coriolis force effects as well as viscosity.
- The instantaneous fiber length is governed by the position of the gravel.
- The fiber diameter is computed from the equation of motion of fiber elements, including viscosity and surface tension effects.
- The temperature of the gravel/fiber ensemble is affected by thermal radiation and convective heat transfer.
- The dynamic viscosity is affected by the instantaneous temperature.
- The fiber formation is terminated when the gravel reaches the high velocity zone of the axial air jets and thus, the gravel/fiber ensemble is displaced from the centrifugal and Coriolis force fields governing the fiber formation.

The most precisely and flexibly controllable technological parameter available at TOPLAN Ltd. at the present state of Junkers technology is the r.p.m. of fiberization disks. For this reason, this paper focuses on the influence of disk speed changes on the fiber geometry. Such tendencies can be most simply demonstrated through the initial droplet size.

The literature (e.g. [14]) is very rich in reporting break-up of moving liquids into droplets. However, no information has been found how the size of a droplet originating from motionless liquid layer can be calculated. For this reason, an own model has been established. *Fig. 6* shows the scheme of a droplet protruding from the melt layer on the fiberization disk (considered to be motionless in the rotating system). The law of motion for the droplet:

$$a = g - \frac{1}{\rho} \text{grad } p, \quad (3)$$

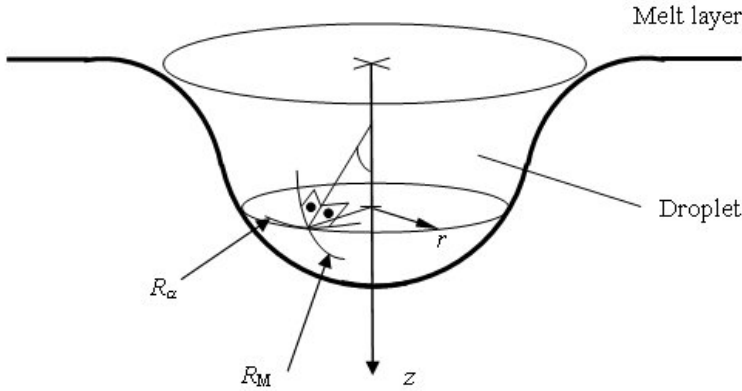


Fig. 6. Scheme of initial droplet

where:  $a$  – acceleration of melt  
 $g$  – intensity of centrifugal force field  
 $\rho$  – melt density  
 $p$  – melt pressure

Expressing the overpressure in the droplet using the surface tension and radii of curvature of droplet surface, the longitudinal component of Eq. (3) reads

$$a_z = g_z - \frac{C}{\rho} \frac{d}{dz} \left( \frac{1}{R_\alpha} + \frac{1}{R_M} \right), \quad (4)$$

where:  $C$  – melt surface tension  
 $z$  – longitudinal coordinate of droplet  
 $R_M, R_\alpha$  – radii of curvature of the meridional and normal sections (see Fig. 6).

$a_z = 0$ , i.e. the law of hydrostatics applies to the motionless, growing droplet before detachment. Fig. 7 shows the droplet at the moment of detachment. Detachment means that the part of droplet closer to the disk – ‘droplet neck’, as marked in Fig. 7 – remains static, however, the part farther from the disk – the actual initial droplet – is accelerated given that the pressure gradient force in the grown droplet can no longer withstand the centrifugal force. This means that the acceleration grows rapidly at a characteristic cross-section of ‘runaway’ where the longitudinal gradient of acceleration will have a maximum (Fig. 7), implying the following conditions

for the runaway cross-section:

$$\frac{d^2(a_z)}{dz^2} = 0$$

and

$$\frac{d^3(a_z)}{dz^3} < 0 \quad (5)$$

The centrifugal force field intensity is the following:

$$g_z = (r_{\text{disk}} + z)\omega_{\text{disk}}^2, \quad \frac{d^2 g_z}{dz^2} = 0 \quad (6)$$

where:  $r_{\text{disk}}$  – radius of fiberization disk  
 $\omega_{\text{disk}}$  – angular velocity of fiberization disk

Expressing  $R_M$  and  $R_\alpha$  as functions of radius  $r(z)$  (see *Fig. 6*), applying conditions (5) to *Eq. (4)*, the resultant differential equation, after reasonable simplifications, leads to the following conclusions regarding the runaway cross-section (*Fig. 7*):

- $dr/dz = 0$  The surface of the droplet is parallel to the  $z$  axis.
- $d^2r/dz^2 = 0$  The surface has an inflexion.
- $d^3r/dz^3 = 0$  This suggests that the meridional curve can be approached as circular arches of equal radius connected at the runaway cross-section. The radius of these arches is the sought  $r_D$  radius of the initial droplet (*Fig. 7*).

Applying the integral form of hydrostatic equation between the  $z = r_D$  and  $z = 2r_D$  points, expressing the pressure difference with use of the surface tension and surface curvatures, and utilizing  $r_{\text{disk}} \gg z$  leads to the final result:

$$r_D = \sqrt{\frac{C}{\rho r_{\text{disk}} \omega_{\text{disk}}^2}} \sim \frac{1}{n_{\text{disk}}} \quad (7)$$

i.e. the size of the initial droplet is inversely proportional to r.p.m. of the fiberization disk  $n_{\text{disk}}$ . Given that the volume of initial droplet is modelled to be in relationship with sum of volumes of gravel and fiber (mass conservation), it has been anticipated that the diameters of gravel and fiber are briefly also inversely proportional to  $n_{\text{disk}}$ . Therefore, the modification of  $n_{\text{disk}}$  was anticipated to be an effectual way of tuning fiber geometry. This anticipation has been justified by technological experiences.

#### 4. Conclusions

Basalt fiber reinforced polypropylene composites have been produced by carding combined with needle-punching and PP fibers were used as carrier fibers. Fracture mechanical tests proved that the treatment of the matrix and the reinforcing

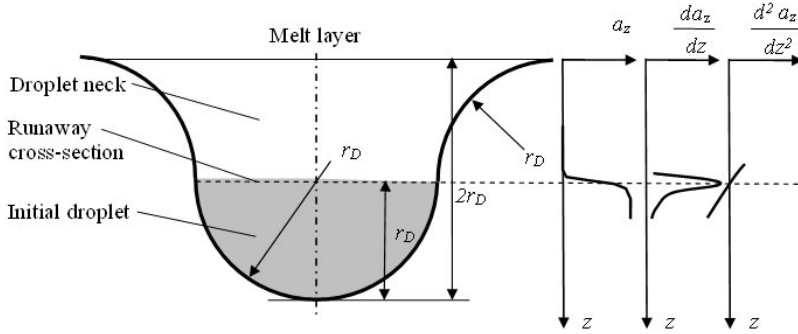


Fig. 7. Time instance of initial droplet detachment

fibers increased the strength of the interfacial adhesion. The scanning electron microscopic analysis of the fracture surfaces of specimens revealed that the gravels formed during fiber production and remaining at the fiber ends increase toughness on the one hand and serve as initiation points of cracks on the other hand. A combined fluid mechanical – thermodynamic model has been outlined for basalt fiber formation in order to provide guidelines in the future how the fiber characteristics can be tuned by means of modification in the technological parameters. A model has been presented for formation of a droplet from a motionless liquid layer. It has been pointed out that the size of initial basalt droplets is inversely proportional to the r.p.m. of the fiberization disks. Therefore, the alteration of disk speed is concluded to be an effectual way of fiber and gravel geometry.

Our results support basalt fiber as a new type reinforcing material of polymer composites and show its spread in advance in the forthcoming years. Basalt fiber can be an alternative for fiberglass since their average density and average tensile elastic modulus are almost the same, and the production cost of basalt fibers is only one half of that of the fiberglass due to the simplicity of the Junkers production technology.

### Acknowledgements

This work was supported by the Hungarian Ministry of Education (NKFP 3/001/2001, TétT JAP-6/00, TétT SF-14/01 and TétT D-16/02).

## References

- [1] GOLDSWORTHY, W. B., New Basalt Fiber Increases Composite Potential, *Compos. Technol.*, **8** (2000), p. 15.
- [2] CHOU, S. – LIN, L. S. – YEH, J. T., Effect of Surface Treatment of Glass Fibres on Adhesion to Phenolic Resin, *Polym. Polym. Compos.*, **7** (1999), pp. 21–31.
- [3] PARK, J. M. – KIM, D. S. – KONG, J. W. – KIM, M. – KIM, W. – PARK, I. S., Interfacial Adhesion and Microfailure Modes of Electrodeposited Carbon Fiber/Epoxy-PEI Composites by Microdroplet and Surface Wettability Tests, *J. Colloid Interf. Sci.*, **249** (2002), pp. 62–77.
- [4] SRIVASTAVA, R. – MEHMED, O., *AIAA J.*, **93** (1993) p. 1634.
- [5] VAD, J. – CORSINI, A., Comparative Investigation on Axial Flow Industrial Fans of High Specific Performance with Unswept and Forward Swept Blades at Design and Off-Design Conditions, *J. 9<sup>th</sup> International Symposium on Transport Phenomena and Dynamics of Rotating Machinery*, Febr. 2002, Honolulu, Hawaii, USA, CD-ROM Proceeding p. 301.
- [6] THOMSON, D. – WATSON, K. – NORDEN, C. – GORRELL, S. – BRAISTED, W. – BROCKMAN, R., *AIAA J.*, **94** (1994), p. 1353.
- [7] GUREV, V. V. – NEPROSHIN, E. I. – MOSTOVOI, G. E., The Effect of Basalt Fiber Production Technology on Mechanical Properties of Fiber, *Glass. Ceram.*, **58** (2001), pp. 62–65.
- [8] BOTEV, M. – BETCHEV, H. – BIKIARIS, D. – PANAYIOTOU, C., Mechanical Properties and Viscoelastic Behaviour of Basalt Fiber-Reinforced Polypropylene, *J. Appl. Polym. Sci.*, **74** (1999), pp. 523–531.
- [9] MAROSI, GY. – ANNA, P. – CSONTOS, I. – MÁRTON, A. – BERTALAN, GY., New Reactive Additives for Interface Modification in Multicomponent Polyolefin Systems, *Macromol. Symp.*, **176** (2001), pp. 189–198.
- [10] CZIGÁNY, T. – MAROSFALVI, J. – KARGER-KOCSIS, J., An Acoustic Emission Study on the Temperature Dependent Fracture Behavior of Polypropylene Composites Reinforced by Continuous and Discontinuous Fiber Mats, *Compos. Sci. Technol.*, **60** (2000), pp. 1203–1212.
- [11] CZIGÁNY, T. – OSTGATHE, M. – KARGER-KOCSIS, J., Damage Development in GF/PET Composite Sheets with Different Fabric Architecture Produced of a Commingled Yarn, *J. Reinf. Plast. Comp.*, **17** (1998), pp. 250–267.
- [12] DUNCAN, W. J. – THOM, A. S. – YOUNG, A. D., *Mechanics of Fluid*, Edward Arnold, 1990.
- [13] LIRNHARD, J. H., *A Heat Transfer Textbook*, Flogiston Press, Cambridge, Massachusetts, USA, 2001.
- [14] *Perry's Chemical Engineers' Handbook*, 6th Edition, McGraw-Hill (1984).